

AD-A106 279

AERONAUTICAL RESEARCH LABS MELBOURNE (AUSTRALIA)  
A DIRECTIONAL SPOTLIGHT BAFFLE FOR CONTROL CABINS, (U)  
OCT 80 K W ANDERSON, B A CLARK  
871 254-00

**F/6 1/5**

UNCLASSIFIED

NL

1 of 1  
2106279

END  
DATE  
FILMED  
1-81  
DTIC

41-81  
NTIC

**LEVEL**

(12)

AD A106279

**DEPARTMENT OF DEFENCE**  
**DEFENCE SCIENCE AND TECHNOLOGY ORGANISATION**  
**AERONAUTICAL RESEARCH LABORATORIES**  
**MELBOURNE, VICTORIA**

SYSTEMS REPORT 22

**A DIRECTIONAL SPOTLIGHT BAFFLE FOR  
CONTROL CABINS**

by

K. W. ANDERSON and B. A. J. CLARK

**DTIC**  
**ELECTED**  
**OCT 29 1981**

A

Approved for Public Release.



THE UNITED STATES NATIONAL  
TECHNICAL INFORMATION SERVICE  
IS AUTHORIZED TO  
REPRODUCE AND SELL THIS REPORT

DTIC FILE COPY

© COMMONWEALTH OF AUSTRALIA 1980

COPY No 11

OCTOBER 1980

81 10 29 025

DEPARTMENT OF DEFENCE  
DEFENCE SCIENCE AND TECHNOLOGY ORGANISATION  
AERONAUTICAL RESEARCH LABORATORIES

SYSTEMS REPORT 22

**A DIRECTIONAL SPOTLIGHT BAFFLE FOR  
CONTROL CABINS**

by

K. W. ANDERSON and B. A. J. CLARK

**SUMMARY**

*Direct overhead lighting in control cabins frequently gives rise to unwanted bright images of the luminaires in the windows and these images may degrade the cabin operator's view of the external world. Opaque louvres or shades and projector-type optical systems have commonly been used in attempts to overcome this difficulty with varying degrees of success. This report describes a directional baffle incorporating light traps which allow a high ratio of wanted to unwanted illumination from a specific conventional spotlight. In practical tests, images from the spotlight-baffle combination were practically inconspicuous both in day and night conditions. A general method of design is described for extension of the principle to other types of spotlamps.*

## DOCUMENT CONTROL DATA SHEET

Security classification of this page: Unclassified

- |  |   |
|--|---|
| 1. Document Numbers                                  | 2. Security Classification                |
| (a) AR Number:<br>AR-002-240                         | (a) Complete document:<br>Unclassified    |
| (b) Document Series and Number:<br>Systems Report 22 | (b) Title in isolation:<br>Unclassified   |
| (c) Report Number:<br>ARL-Sys-Report-22              | (c) Summary in isolation:<br>Unclassified |

3. Title: A DIRECTIONAL SPOTLAMP BAFFLE FOR CONTROL CABINS

- |  |                                    |
|--|------------------------------------|
| 4. Personal Authors:<br>Anderson, K. W.<br>Clark, B. A. J. | 5. Document Date:<br>October, 1980 |
| 6. Type of Report and Period Covered:                      |                                    |

- |  |   |
|--|---|
| 7. Corporate Author:<br>Aeronautical Research Laboratories | 8. Reference Numbers<br>(a) Task: DST 76/151<br>(b) Sponsoring Agency: DSTO |
| 9. Cost Code: 73 4401                                      |   |

- |  |  |
|--|--|
| 10. Imprint:<br>Aeronautical Research Laboratories,<br>Melbourne | 11. Computer Program(s)<br>(Title(s) and language(s)): |
|--|--|

12. Release Limitations (of the document): Approved for Public Release

12.0. Overseas:	N.O.	P.R.	1	A		B		C		D		E	
-----------------	------	------	---	---	--	---	--	---	--	---	--	---	--

13. Announcement Limitations (of the information on this page): No limitation

- |                           |                        |
|---------------------------|------------------------|
| 14. Descriptors:          | 15. Cosati Codes: 1301 |
| Human factors engineering | Glare 0105             |
| Veiling reflection        | Light control 0505     |
| Baffles                   | Airport towers 2006    |
| Illuminance               |                        |

16. **ABSTRACT**

*Direct overhead lighting in control cabins frequently gives rise to unwanted bright images of the luminaires in the windows and these images may degrade the cabin operator's view of the external world. Opaque louvres or shades and projector-type optical systems have commonly been used in attempts to overcome this difficulty with varying degrees of success. This report describes a directional baffle incorporating light traps which allow a high ratio of wanted to unwanted illumination from a specific conventional spotlight. In practical tests, images from the spotlight-baffle combination were practically inconspicuous both in day and night conditions. A general method of design is described for extension of the principle to other types of spotlamps.*

## CONTENTS

	Page No.
1. INTRODUCTION	1
2. LIGHTING REQUIREMENTS FOR THE FLYING CONTROL CABIN	1
2.1 Cabin Window Reflections	1
2.2 Overhead Lighting	1
2.3 Characteristics of the Lamp	2
2.4 Characteristics of the Shade	3
3. DEVELOPMENT OF THE SPOTLAMP BAFFLE	3
3.1 Conventional Methods of Shading	3
3.2 Light Traps	3
3.3 Internal Edges	4
3.4 Umbral and Penumbral Regions	4
3.5 Design Compromises	5
4. PHOTOMETRIC CRITERIA	6
4.1 Brightness Contrast	6
4.2 Angle Effect	7
4.3 Ideal Baffle Performance	7
5. PHOTOMETRIC EXPERIMENTS	8
5.1 Apparatus	8
5.2 Voltage Effect	9
5.3 Angle Effect	10
6. DISCUSSION	10
7. CONCLUSIONS	11
REFERENCES	
SYMBOLS	
FIGURES	
APPENDIX A—Geometry of the Spotlamp Baffle	
APPENDIX B—Characteristics of the PAR 38 Spotlamp	
APPENDIX C—Photographs of Lamp, Shades and Rings	
DISTRIBUTION	

A	
Approved for Release	
by NSA/CSSA	
on 08/14/2013	
Special	

## 1. INTRODUCTION

Overhead lighting (i.e. lighting from overhead luminaires) is used for the great majority of workplaces. Tasks such as reading and writing at a desk are often done with illumination provided solely by the overhead lighting system used for general room illumination. Sometimes it is advantageous to provide increased illumination in certain parts of the room; this may be done with local light sources such as desk or reading lamps or with a more directional type of luminaire (e.g. spotlamps) which for convenience may be mounted on a nearby wall or ceiling.

This Report is about a directional luminaire which has only a minute proportion of its luminous output outside its main beam. The luminaire consists of a commercial spotlamp together with a cylindrical baffle attachment which was devised at ARL originally for use in the flying control cabin (known colloquially as 'Flyco') of the aircraft carrier *HMAS Melbourne*. Light is required in that cabin for reading, writing, seeing instruments and operating controls and communication equipment. At night, the cabin operators need to be able to see the dim external scene without hindrance from the cabin lighting—either as disability glare or as reflections in the windows.

Satisfactory resolution of these apparently conflicting requirements for Flyco was achieved by using the directional luminaire in conjunction with some internal lighting of instruments and pushbuttons (Ref. 1).

A method for designing a directional baffle is given in Section 3. This method is readily adaptable to the design of lighting systems in air traffic control tower cabins, on ships' bridges, in railway and crane control cabins and in other situations where operators need panel or desk illumination with minimal degradation of their external view. Other applications for a spotlamp with little off-axis illumination seem likely for searchlights, landing lights, in television and photographic studios, art galleries and intruder detection systems for example.

## 2. LIGHTING REQUIREMENTS FOR THE FLYING CONTROL CABIN

The characteristics of the spotlamp and baffle were chosen to suit the Flyco application. Relevant aspects of Flyco workspace layout are described in this section as a basis for any adaptation of the design for other applications.

### 2.1 Cabin Window Reflections

Figure 1 shows a workspace arrangement in which an unwanted image of a luminaire falls in an operator's field of external view. By day and by night these images (and images of other objects in the cabin) may cause confusion, glare or masking of objects in the external scene.

Windows in Flyco and some other control cabins slope outwards at the top. This allows a better downwards view from close to the window, but objects in the upper part of the cabin interior can then cause unwanted images overlying the external field of view around and above the horizontal direction. If those objects are moderately dark (as a result of dim illumination of poorly reflective surfaces), then those images will be relatively faint. However, cabins with light-coloured ceilings and unshielded luminaires (e.g. exposed fluorescent tubes) will tend to have relatively prominent images in their windows.

### 2.2 Overhead Lighting

In the case of Flyco, lighting from overhead luminaires instead of desk lamps was chosen as the principal means of workspace illumination on the basis of trials in a full-scale wooden

mock-up of the cabin. The advantages demonstrated were:

- (i) the illumination throughout the cabin was relatively more even, and this allowed the overall level to be much lower in the interest of external vision while still providing enough light for safe movement in the cabin;
- (ii) legends and controls on the control panels were more easily seen than when illuminated only by stray light from nearby local desk lighting and from internally lit instruments and switches;
- (iii) unlike the situation with local desk light fittings, desk activities and external visual fields were not impeded by the overhead lighting;
- (iv) useful reduction of out-in adaptation time seemed attainable with the facility of flood-lighting the workspace when the external scene was in bright daylight (Ref. 2); and
- (v) the better uniformity of desk and panel illumination was subjectively rated to be more satisfactory for operator comfort and orientation.

Several types of commercially available overhead luminaires were tried. All produced unacceptably bright reflections in the cabin windows. Reference 3 suggests the elimination or control of glare by suitable baffles or shades, but even when the best of the luminaires was improved by fitting a commercially available louvre baffle to improve shielding and directionality, it was still far from acceptable.

In seeking a light source with better directional qualities, a projector-type spotlight was considered. These devices have an illuminated aperture (or 'gate') which is imaged by an objective lens onto a workplace. Movable edges of the gate allow adjustment of the size and shape of the illuminated area, as in some theatre 'follow spots'.

In addition to being expensive, the projector spotlamps considered were mostly too large in physical size for use on the relatively low ceiling of the Flyco cabin. The smaller units had insufficient luminous output for effective use in Flyco's daylight operations, as in (iv) above. All of these units had their objective lenses visible to as much as 80° from the axis. Stray light from multiple reflections and lens imperfections would render unshaded projectors unsuitable for this application. Because an effective shade was expected to add substantially to their already excessive length, projector spotlamps were considered no further.

### 2.3 Characteristics of the Lamp

Four Phillips PAR 38 pressed-glass lamps ('spot' rather than 'flood' type), each rated at 150 W, were judged in practical trials to be the most suitable for overhead lighting in the Flyco cabin for the following reasons.

- (a) Each lamp produces most of its useful illumination in a cone within  $\pm 15^\circ$  of its axis. This seemed appropriate for the given desk-to-panel width and desk-to-ceiling distance.
- (b) With four lamps, the cones of light could be arranged to give sufficiently uniform illuminance over the desk region.
- (c) A useful output of about 1600 lumen per lamp (providing an illuminance of over 300 lux at 1.5 m) was thought necessary to provide sufficient supplementary illumination in daylight conditions.
- (d) The luminous output of incandescent lamps such as the PAR 38 type can be readily reduced for night-time use by voltage reduction. This is accompanied by a reduction in colour temperature which has some advantages for visual comfort and dark adaptation of the human visual system at night (Ref. 4).
- (e) The PAR 38 lamp is available with a dichroic reflector which transmits near infrared radiation and thereby reduces the heating effect of the light beam with little effect on its colour or quantity.

- (f) Having a relatively small emitting face (about 100 mm diameter), the PAR 38 can be shaded more easily than lamps of larger diameter.

Further specifications of the PAR 38 lamp can be found in Appendix B.

#### 2.4 Characteristics of the Shade

The purpose of the lamp shade is to reduce the amount of stray light escaping from the overhead PAR 38 spotlight with minimal interference with its  $\pm 15^\circ$  cone of useful illumination. For the chosen luminaire positions in the Flyco cabin, stray light outside a  $\pm 35^\circ$  cone could illuminate the windows and cause the reflection problem described in Section 2.1 above. Consequently  $35^\circ$  was chosen in the shade design as the maximum off-axis angle for direct ray paths from the lamp face passing outside the shade. This angle is called the cut-off angle,  $\gamma$ .

Practical trials in the cabin mock-up were used to give an indication of the maximum length of shade that could be used without encroaching too much into the already limited standing headroom. Obviously if there were no limit at all, the shade could extend right down to the desk and there give a sharp cut-off to the illuminated area. On the other hand, if the lower end of the shade is constrained to be too close to the lamp, it is not possible to intercept enough of the off-axis unwanted light unless the aperture is made smaller than the emitting face of the lamp. This would be wasteful of the available light and rectification would require a smaller lamp and a compensating increase in the number of luminaires.

A shade length of 180 mm and a circular aperture of 100 mm diameter (yielding a cut-off angle of about  $35^\circ$ ) was deemed to be an acceptable compromise between several competing factors: headroom required; extent, quantity and evenness of workspace illumination; and the cut-off angle between illuminated and shaded regions.

The final characteristic demanded of the shade pertains to stray light rays outside the cut-off angle. These result from reflection and/or diffraction of source rays by the inner surface of the shade. Because performance is inversely related to the amount of stray light, the inner surface should have a form having a small total reflectance.

### 3. DEVELOPMENT OF THE SPOTLAMP BAFFLE

#### 3.1 Conventional Methods of Shading

Conventional methods for limiting off-axis illumination include the use of shades and louvre devices as shown in Figure 2. Shades are usually cylindrical or conical in shape; louvres can have linear, grid or cylindrical elements. The effectiveness of these is related to the light absorbing properties of the inner surfaces of the device. Even with materials having unusually small total reflectances (such as black flock paper and black velvet), as much as 1% of the incident light may be reflected. A cylindrical shade with an inside lining of clean black flock paper was tried in the Flyco mock-up: the window reflections were still unacceptably bright. Therefore, it appears that any arrangement which allows the light to escape after just one reflection, even from clean black flock paper, could be unsatisfactory. Furthermore, black flock paper and black velvet are notoriously difficult to keep clean and deposits of airborne dust soon degrade the special light absorbing properties of that type of material.

#### 3.2 Light Traps

The amount of unwanted escaping light can be reduced by the use of light traps. As shown in Figure 3, the increased attenuation is physically the result of two, three or more reflections rather than one.

If the surfaces are each painted matt black and have a total reflectance of about 4%, the ratio of reflected to incident light for each emerging ray is less than  $(0.04)^k$  where  $k$  is the number of reflections undergone by that ray. Overall reflectance will be less than  $(0.04)^2$  or  $1.6 \times 10^{-3}$ . If the surfaces are black gloss, specular reflections will tend to predominate rather than diffuse reflections and emerging rays will mostly have undergone three or more reflections so that the overall reflectance will be less than  $(0.04)^3$  or  $6.4 \times 10^{-5}$ .

The rationale of the light trap is that no element of the surface visible to the observer should



be illuminated directly by the source. The glare stops used in ancient and modern telescopes are usually placed according to a similar criterion. The geometrical arrangement for the inner surface of a cylindrical shade is shown in Figures 4, 5 and 6. In this Report, a shade fitted with light traps is called a baffle. It is shown in Appendix A that the cut-off angle,  $\gamma$ , is given by

$$\gamma = \arctan \left( \frac{W + D}{2H} \right), \quad (1)$$

where  $W$  is the baffle diameter,  $H$  is the baffle length and  $D$  is the lamp diameter. It is further shown that the spacing between adjacent ring stops must be no more than

$$S = \frac{TH}{W}, \quad (2)$$

where  $T$  is the ring stop width, in order to prevent observation of rays which have undergone just one reflection (viz. reflection from the inner shade surface only).

The minimum number of spacings,  $N$ , is found by evaluating  $W/T$  and rounding up to the next integer. Should that ratio be integer, then

$$N = \frac{W}{T}. \quad (3)$$

The number of ring stops is  $(N - 1)$ .

### 3.3 Internal Edges

For a baffle of cylindrical external shape, the light trap stops were initially envisaged as flat rings cut from sheet material, as shown in Figure 5. The cross section of the rings would be rectangular of small but finite thickness. The inner faces of these rings would then perform like the inner surface of a cylindrical shade without light traps: reflections, both specular and diffuse, from these inner faces could occur as shown in Figure 7. As a result, light from the source could be directed outside the cut-off angle after just one reflection. Although only a small fraction of the total luminous flux could be so directed, the performance would nevertheless be degraded below that of ideal light traps (i.e. perfectly black stops with optically sharp edges).

This effect will be reduced towards the limit set by diffraction if the internal face is machined to a sufficiently sharp edge. Figure 8 shows the angles  $\alpha_1$  and  $\alpha_2$  which should be smaller than the path angles  $\beta_1$  and  $\beta_2$  in order to optimise the light trap effect. Using the geometrical analysis derived in Appendix A, the following are upper limits for  $\alpha_1$  and  $\alpha_2$  for each ring stop:

$$\alpha_1 = \arctan \frac{n}{N} \left( \frac{H}{W - T} \right) \quad (4a)$$

and

$$\alpha_2 = \arctan \left( 1 - \frac{n}{N} \right) \left( \frac{2H}{W - 2T + D} \right) \quad (4b)$$

where the rings are numbered

$$n = 1, 2, \dots, (N - 1)$$

as shown in Figure 8.

### 3.4 Umbral and Penumbral Regions

Figure 9 shows the outer edge of the illuminated penumbral region as defined by the cut-off angle,  $\gamma$ . Concentric within that region is the umbral region which can be illuminated by the entire lamp face. Its boundary is defined by the angle  $\psi$  as shown.

For a given  $\{H, W, \gamma, D\}$  the value of  $\psi$  can be altered somewhat by the choice of number, size and spacing of ring stops, but  $\psi$  cannot exceed  $\gamma$ . As an indicator of the relative sizes of

cones, it is convenient to define the Penumbral Factor,  $\eta$ , as

$$\eta = \frac{\tan \psi}{\tan \gamma} \quad (5)$$

A relatively large value of  $\eta$  (approaching unity) would imply a relatively large umbra and a narrow penumbra; i.e. a sharp cut-off.

A zero value of  $\eta$  would imply a zero value for  $\psi$ ; i.e. the umbral region would be a cylinder centred on the lamp axis and with a diameter equal to the diameter of the lamp face. A negative value of  $\eta$  would imply a negative value of  $\psi$  which could only occur in practice if the outermost ring stop had an internal diameter smaller than the diameter of the emitting face of the lamp and if the remaining ring stops had internal diameters which increased with decreasing distance from the lamp so as to avoid vignetting of the extreme umbral rays. In the case of negative  $\eta$ , the umbral region of illumination extends only for a finite distance from the lamp, viz. to the distance where the extreme umbral rays intersect on the lamp axis. Absorption of useful light by the baffle is greater as  $\eta$  tends towards negative values.

The Penumbral Factor will therefore be an indication of the geometrical efficacy of the baffle for a given cut-off angle. In Appendix A, it is shown that if (2) and (3) are satisfied,

$$\eta = \frac{1 - D/W - 2/N}{1 + D/W - 2/N} \quad (6)$$

A graph of  $\eta$  is given in Figure 10. It is clear that larger values of  $N$  and smaller values of  $D/W$  are conducive to larger values of  $\eta$ . However, the improvement in  $\eta$  for increasing  $N$  is progressively less (i.e., a diminishing return situation).

### 3.5 Design Compromises

The layout and orientation of the workplace, windows, observers, etc., will indicate the preferred values for the cut-off angle,  $\gamma$ , and the total baffle length,  $H$ . The term  $(2H \tan \gamma)$  can then be evaluated. From Equation (1), this term should be equal to  $(W - D)$ , and therefore should be considered when seeking a suitable lamp.

Lamp characteristics—including directionality (illustrated by its intensity polar diagram), total output, suitability for dimming, availability and practicability—will further constrain the lamp choice. Of those eligible, the lamp with the smallest emitting face should be chosen as this will yield the most favourable Penumbral Factor. Lamp diameter,  $D$ , will then be known and so  $W$  may be calculated using equation (1). Should it not prove possible to find a suitably small lamp, a larger lamp and a larger baffle (i.e., a larger value of  $H$ ) should be considered.

Rearranged workspace, different luminaire positions or recessed luminaires may allow a longer baffle.

After the iterative procedure above has identified the compromise which is most satisfactory to the designer,  $\{H, W, D, \gamma\}$  will have been defined.

The number of spacings,  $N$ , or ring stops,  $(N - 1)$ , will determine the ring stop width,  $T$ , and inter-stop spacing,  $S$ , if equations (3) and (2) are used. Although more rings would increase the Penumbral Factor, more manufacturing expense would be incurred. Moreover, because diffraction at each internal edge produces some stray light, the number of rings has also to be a compromise between a large number for good geometrical efficacy and a small number for the smallest amount of stray light.

Consequently, it was judged for the present purpose that the number of spacings,  $N$ , should be selected from the range four to ten. In other cases, values near four or less may be a suitable compromise when minimising stray light is considered particularly important, or when a very low  $D/W$  ratio is used. Values near ten may be considered more suitable when a relatively large umbra is required.

Finally, equation (4) can be used to derive the upper limits for the angles on the inner surfaces of the ring stops. For ease of manufacture, some standardisation of ring angles may be preferred. This would result in the use of angles less than those calculated. Acute angled edges

should be avoided because of their greater susceptibility to damage in manufacture and service, as well as the greater potential injury hazard if the edges are sharp.

#### 4. PHOTOMETRIC CRITERIA

##### 4.1 Brightness Contrast

Consider an arrangement where an overhead light source is used to illuminate a specific area near a window. If that window is used for external viewing, an unwanted image may be generated as shown in Figure 1. For the practical avoidance of this problem, the image superimposed on the background should be fainter than the visual detection threshold for those conditions of observation.

The horizon sky luminance is known to vary from about  $10^{-4}$  cd m<sup>-2</sup> on dark moonless overcast nights to about  $10^4$  cd m<sup>-2</sup> on clear sunny days (Ref. 5). If  $B_s$  is the luminance of sky background and  $B_i$  is the luminance of the just distinguishable superimposed image, then the threshold of brightness contrast ( $\epsilon$ ) is given by:

$$\epsilon = \frac{B_i}{B_s} \quad (5)$$

Experiments with a large number of observations (Ref. 5) have established that  $\epsilon$  is a function both of background luminance and of image size, as shown in Table 1.

Unfortunately, published threshold contrast data mostly refer to disk-shaped targets, and while those data can be applied to square targets or other compact shapes of similar area with some justification, extension of the data to the complex luminance distribution of the baffle image appears to be beyond validity. Seen from the cut-off area (i.e.  $\theta \geq \gamma$ , Figures 1 and 2) the image consists of an ellipse (which is the foreshortened circular exit pupil of the baffle) through which can be seen illuminated elliptical arcs (the diffracting edges of the ring stops) overlying the light traps which are generally much fainter than the arcs. The effort required to gain threshold contrast data for this special case would appear to be incommensurate with the value of the results. As a crude but much easier alternative, consider the approximation that the intensity of the baffle exit pupil seen from the cut-off area arises from a uniform luminance across the exit pupil area. For the image to be invisible according to this approximation, its luminance  $B_i$  must satisfy

$$B_i \leq \epsilon B_s, \quad (6)$$

where  $\epsilon$  is the threshold contrast appropriate to a disk of solid angle equal to the solid angle of the exit pupil seen by the observer. In practice (and this has been confirmed by observation), the non-uniform distribution of luminance could be expected to result in the brighter parts of the image being above threshold when  $B_i = \epsilon B_s$ . However, the image as a whole is inconspicuous in practical terms, and inequality (6) is thus more properly a criterion for inconspicuity.

**TABLE 1**  
**Thresholds of brightness contrast,  $\epsilon$ , for various levels of background**  
**luminance and stimulus diameter**

(Derived from graphs of H. R. Blackwell's data  
Fig. 5.3 in Reference 5)

Disk target stimulus diameter arc minutes	Background luminance (cd m <sup>-2</sup> )				
	$10^{-4}$	$10^{-2}$	$10^0$	$10^2$	$10^4$
360	0.079	0.020	0.0045	0.0028	0.0028
121	0.18	0.030	0.0056	0.0028	0.0028
55	0.32	0.045	0.0063	0.0028	0.0028

## 4.2 Angle and Voltage Effects

If  $A$  represents the cross-sectional area of the baffle exit pupil, then the foreshortened area seen by the observer is given by:

$$\text{visible area} = A \cos \theta. \quad (7)$$

The intensity of the image is that of the source attenuated by the window reflectance,  $R$ . Consequently, the image luminance is given by:

$$B_I = \frac{R I_{\theta,V}}{A \cos \theta}, \quad (8)$$

where  $I_{\theta,V}$  is the intensity of the source in the given direction,  $\theta$ , at a given voltage,  $V$ .

The effects of  $\theta$  and  $V$  on  $I_{\theta,V}$  are independent (except for small effects of no practical consequence arising from interaction of the spectral characteristics of the lamp filament and reflector) and so a voltage factor and an angle factor can be defined:

$$I_{\theta,V} = I_{\max} F_{\theta} F_V, \quad (9)$$

where  $I_{\max}$  is the lamp intensity at rated voltage along the lamp axis.  $F_{\theta}$  (a function of  $\theta$ ) is a characteristic of the lamp and baffle combination.  $F_V$  (a function of  $V$ ) is characteristic of the particular lamp.

Combining equations (6), (8) and (9) produces the following:

$$\frac{R I_{\max} F_{\theta} F_V}{A \cos \theta} \leq \epsilon B_s,$$

which can be arranged to:

$$\frac{F_{\theta} F_V}{\cos \theta} \leq \frac{\epsilon B_s A}{R I_{\max}}.$$

Therefore the condition for inconspicuity reduces to

$$\frac{F_{\theta} F_V}{\cos \theta} \leq \frac{\epsilon B_s}{R B_{\max}}, \quad (10)$$

where  $B_{\max}$  is the lamp's luminance at its rated voltage along its axis (i.e.  $I_{\max}/A$ ). The design aim is for (10) to be satisfied in the cut-off region where

$$\theta \geq \gamma.$$

## 4.3 Ideal Baffle Performance

The PAR 38 incandescent spotlight (described in Appendix B) has a maximum luminance at its emitting face of approximately  $6 \cdot 10^5 \text{ cd m}^{-2}$ . Window transparencies, like glass or perspex, have a reflectance of about 4% for each surface for incidence angles of less than  $60^\circ$ . Consequently, the value of 0.08 is used for  $R$ . Other parameters in inequality (10) depend upon the prevailing luminous conditions which can vary markedly. The two extreme conditions are considered below.

### (a) Daylight

Values of  $10^4 \text{ cd m}^{-2}$  and 0.003 are used for  $B_s$  and  $\epsilon$  respectively (see Section 4.1) as representative of bright daylight conditions. After substitution, inequality (10) becomes

$$\frac{F_V F_{\theta}}{\cos \theta} \leq 6.25 \cdot 10^{-4}. \quad (11)$$

If the lamp is operating at rated voltage,  $F_V$  equals unity, and therefore for inconspicuity when  $\theta$  exceeds  $\gamma$ ,

$$\frac{F_{\theta}}{\cos \theta} \leq 6.25 \cdot 10^{-4}. \quad (12)$$

### (b) Night-time

As cited in Section 4.1, a value of  $10^{-4} \text{ cd m}^{-2}$  is suitable for  $B_s$  on a very dark night. From Table 1, the most conservative value of  $\epsilon$  is 0.079. Larger values are applicable to smaller stimuli. After substitution, (10) becomes

$$\frac{F_v F_n}{\cos \theta} \leq 1.6 \times 10^{-10}, \quad (12)$$

i.e. an attenuation of about 10 orders of magnitude is required. Because illumination levels required at night are less than during the day - especially where a degree of dark adaptation is required for the operator's eyes - a small value of  $F_v$  should be expected for night conditions. However, from experiments in the mock-up it seems unlikely that an  $F_v$  value of less than  $10^{-4}$  would allow enough light for visual tasks within Flyco and similar cabins and consequently it would be desirable for the angle effect (i.e.  $F_n \cos \theta$ ) to contribute an attenuation of at least six orders of magnitude for angles greater than the design cut-off angle. Therefore it is desired that

$$\frac{F_n}{\cos \theta} \leq 1 \times 10^{-6} \quad (13)$$

for all values of  $\theta$  greater than  $\gamma$ .

From the above it appears that the night-time criterion (13) is the more demanding and should be used in the design or selection of a suitable baffle. For best use of the available light near the baffle axis, no attenuation should occur for angles less than the design cut-off angle, and therefore the ideal angle effect is described as:

$$\log \left( \frac{F_n}{\cos \theta} \right) = 0 \text{ for } \theta \leq \gamma \quad (14a)$$

and

$$\log \left( \frac{F_n}{\cos \theta} \right) \leq -6 \text{ for } \theta > \gamma. \quad (14b)$$

This is shown in Figure 13. In practice with a cylindrical shade or baffle, vignetting results in the penumbral region shown in Figure 9 not being illuminated as brightly as the umbral region, so accounting for part of the difference between ideal and actual performance. The actual curves in Figure 13 are based on the experimental work described in the following section.

## 5. PHOTOMETRIC EXPERIMENTS

### 5.1 Apparatus

All of the experimental work described in this section used a single Philips PAR 38 dichroic lamp as described in Appendix B. The lamp was fitted in a 'Quad Minor' lamp housing which is a die-cast metal fitting made by the Kempthorne Lighting Company (catalogue number K 7141). This housing contains attachment points for a shade or baffle.

Three attachments were evaluated: a commercial 'anti-dazzle screen' and two prototype baffles developed at ARL within the design guidelines given in Section 3 and using the parameters listed in Table 2. The internal angles of the ring stops are given in Table 3.

Prototype A used ring stops of approximately 2.5 mm thickness with the inner surface turned to provide the desired angles given in Table 3. Prototype B used thinner rings of about 1.25 mm thickness: these were cut from sheet material, pressed in a die (to provide the 30° surface) and then machined in a lathe (to provide the 10° surface). The resulting sections are shown in Figure 11. The cylindrical shades were fabricated from sheet aluminium over most of their length. The outer rim of both prototypes was of black neoprene rubber to minimize injury potential. Both sets of ring stops were made from an aluminium alloy with a relatively high magnesium content; this alloy was chosen for its turning and edge-keeping qualities. Appendix C contains photographs of the lamp, shades and rings. Specifications of Prototype B are detailed in Garden Island Dockyard Drawing No. 534 225 (26 February 1979).

**TABLE 2**  
**Parameters of ARL prototype baffles**

Description	Symbol	Dimension
Lamp effective diameter	$D$	100 mm
Effective length	$H$	180 mm
Width overall	$W$	150 mm
Ring stop width	$T$	25 mm
Ring stop spacing	$S$	30 mm
Number of ring stops	$N - 1$	5
Cut-off angle	$\gamma$	35°
Penumbra Factor	$\eta$	0

**TABLE 3**  
**Angles of the internal ring stops**

Ring stop number  $n$	Angles of internal edges of ring stops (degrees)					
	Computed Maximum*		Selected for Prototype A†		Selected for Prototype B†	
	$\alpha_1$	$\alpha_2$	$\alpha_1$	$\alpha_2$	$\alpha_1$	$\alpha_2$
5	50.2	16.7	50	10	30	10
4	43.8	31.0	40	20	30	10
3	35.8	42.0	30	30	30	10
2	25.6	50.2	20	40	10	30
1 (farthest from lamp)	13.5	56.3	10	50	10	30

\* Computed using equations (4a) and (4b) and the parameters of Table 2.

† Selected for ease of manufacture.

All photometric measurements were made in the ARL Vision Laboratory using a Pritchard Photometer (Model 1980, Serial A119). The photometer objective lens was located 3.75 m from the lamp emitting face and a measuring field of 3.2° was used. The results were subsequently confirmed using a viewing distance of 9.3 m and a measuring field of 1°. Decade changes to the photometer's sensitivity were made by using appropriate combinations of:

- (i) photometer aperture restriction;
- (ii) neutral density filters; and
- (iii) electronic attenuation.

## 5.2 Voltage Effect

The lamp was mounted facing the photometer in a darkened room. In order to achieve accurate alignment both lamp and photometer were adjusted in azimuth and elevation to give a maximum photometer luminance reading.

The lamp was connected through an adjustable autotransformer ('Variac') to a stabilised 230 V supply. The lamp voltage was monitored with an analogue 'AVO' voltmeter.

The voltage was adjusted in ten-volt increments downwards from the rated voltage. Photometer readings of luminance with no filter, with the red filter and with the blue filter were recorded as  $B_V$ ,  $B_{red}$  and  $B_{blue}$  respectively. From these readings, the following data were calculated for each voltage:

- (i) the lamp intensity along its axis,  $I_V = B_V A_d$ , where  $A_d$  is  $0.034 \text{ m}^2$ , the area of the photometer's circular measuring field subtending  $3.2^\circ$  at  $3.75 \text{ m}$ ;
- (ii) the Intensity-Voltage Factor,  $F_V = I_V/I_{max}$ ;
- (iii) the blue/red ratio  $= B_{blue}/B_{red}$ ; and
- (iv) the colour temperature from the blue/red ratio using the curve calibrated by the photometer manufacturer.

Figure 12 shows a graphical record of the results.

### 5.3 Angle Effect

The lamp was operated at a constant voltage of 230 V.

The lamp was mounted in a fitting which had been adapted to provide measurable adjustment in elevation angle. The zero position of the angular scale was calibrated using an inclinometer. The photometer axis was aligned with the zero angle line. Lamp luminance was measured for viewing angles to  $90^\circ$  in  $5^\circ$  increments. These measurements were first made with the lamp and fitting without any baffle and were then repeated for each baffle.

Using the measured luminance  $B_\theta$  for each viewing angle  $\theta$ , the following data were calculated:

- (i) the intensity in the given direction,  $I_\theta = B_\theta A_d$ ;
- (ii) the Intensity-Angle Factor,  $F_\theta = I_\theta/I_{max}$ ; and
- (iii) for comparison with other baffles,  $\log\{F_\theta/\cos \theta\}$ .

The results are shown graphically in Figure 13.

## 6. DISCUSSION

It is desired that useful illumination be available on and near the lamp axis and that simultaneously the off-axis aspect of the lamp be practically invisible to an observer. It was shown in Section 4 that this objective demands that the off-axis luminance be about six orders of magnitude less than the on-axis luminance. Further, it is desired that the transition from no attenuation to full attenuation should occur over a small range of viewing angles in the region of the chosen cut-off angle,  $\gamma$ . Therefore the gradient of  $F_\theta$  versus  $\theta$  curve should be greatest where  $\theta$  is near  $\gamma$  and relatively small elsewhere.

It is clear from Figure 13 that both the PAR 38 lamp alone and the PAR 38 lamp with a conventional louvre shade provide a steady decrease in the luminance as the viewing angle is increased. At  $75^\circ$ , the attenuation reaches about three and four orders of magnitude respectively. For control cabin applications like Flyco, this is not good enough.

For each of the prototype baffles described in Section 5, the design cut-off angle was  $35^\circ$ . The experimental results plotted in Figure 13 show that an attenuation of 5.5 orders of magnitude was achieved for viewing angles greater than  $50^\circ$ . No further improvement was evident at greater angles. Experimentally, this is very close to the physical limit set by diffraction for the given number of rings (as a new razor blade edge appeared comparably as bright as a similar length of a ring edge). Further improvement would require a reduction in the number of rings but this would require an increase in the baffle dimensions and/or a decrease in the Penumbra Factor.

For angles between  $10^\circ$  and  $35^\circ$  (in the penumbra) the baffles provided some unwanted attenuation. As desired, the gradient  $dF_\theta/d\theta$  is greatest when  $\theta$  is near  $35^\circ$ . In the region of  $35^\circ$  to  $50^\circ$ , attenuation was less than desired even though the lamp face was no longer visible. Light scattering by the atmospheric aerosol, and diffraction and specular highlights from the sharp

ring edges seemed to be the main mechanisms. The two prototypes exhibited similar performance over the entire angular range. Although Prototype A generally provided more attenuation, the two curves in Figure 13 are close together. More detail is shown in Figure 14. Because this difference is so small, it is considered that any choice between the two prototypes should be made on other criteria.

Subjectively it was considered by several observers with control cabin experience that both prototypes were successful in providing adequate night-time desk illumination without a discernable window image of the lamp against a black background. The highlights from the baffle ring edges were visible but were considered inconspicuous. In simulated daylight conditions also the system was considered effective.

In production it may be possible to make several economical changes from the prototypes without any practical reduction in performance. For example, an opaque plastic moulding may be suitable for the outer cylindrical shade.

Finally, beam shaping by the use of non-circular apertures appears feasible and could sometimes be of considerable value. The foregoing design technique can be applied to appropriate axial sections, thereby allowing a practical arrangement to be formulated.

## 7. CONCLUSION

The need for an effective directional spotlight baffle has been described. A suitable baffle has been devised, a method of design has been developed and prototypes have been made and tested.

Experimental results and subjective evaluations confirm that the new baffle meets the performance characteristics required. For control cabins, baffles designed with the method described will allow spotlights mounted in appropriate positions on walls or ceilings to be used for workspace illumination without the disadvantage of unwanted conspicuous reflections in the windows.



## REFERENCES

1. Anderson, K. W. *An ergonomic design for the Flying Control Position on HMAS Melbourne*. Aeronautical Research Laboratories, Melbourne, Systems Report 18, 1980.
2. Clark, B. A. J. *A brief appraisal of visual problems in Air Traffic Control facilities used by service aircraft*. Aeronautical Research Laboratories, Melbourne, Systems Technical Memorandum 32, 1972.
3. Standards Association of Australia. *Interior Lighting and the Visual Environment*. AS 1680-1976.
4. Kruithof, A. A. Tubular luminescence lamps for general illumination. *Philips Technical Review*, 6, 65-73, 1941.
5. Middleton, W. E. K. *Vision through the Atmosphere*. Toronto: University of Toronto Press, 1952.

## SYMBOLS

$A$	Cross-sectional area of lamps
$A_d$	Area of photometer measuring disk
$B_{\text{blue}}$	Lamp luminance as measured through photometer's blue filter
$B_I$	Image luminance in a given direction
$B_{\text{max}}$	Lamp luminance along its axis at rated voltage
$B_{\text{red}}$	Lamp luminance as measured through photometer's red filter
$B_s$	Sky luminance
$B_V$	Lamp luminance along its axis for a given voltage
$B_\theta$	Lamp luminance at rated voltage in a given direction
$D$	Lamp diameter
$F_V$	Intensity Voltage Factor $I_V/I_{\text{max}}$
$F_\theta$	Intensity Angle Factor $I_\theta/I_{\text{max}}$
$H$	Baffle length
$I_{\text{max}}$	Lamp intensity at rated voltage along its axis
$I_V$	Lamp intensity along its axis for a given voltage
$I_\theta$	Lamp intensity at rated voltage in a given direction
$I_{v,v}$	Lamp intensity as a function of $\theta$ and $V$
$N$	Number of spaces between ring stops
$R$	Reflectance of window transparency
$S$	Axial distance between ring stops
$T$	Radial width of ring stops
$V$	Voltage applied to lamp
$W$	Internal diameter of baffle outer case
$\alpha$	Angles of internal edges of ring stops
$\beta$	Angles of rays at ring stops
$\gamma$	Cut-off angle
$\epsilon$	Threshold for brightness contrast
$\eta$	Penumbra Factor
$\theta$	Angle between baffle axis and light path to observer from the lamp/baffle exit aperture
$\phi$	Angle between baffle axis and light path from source
$\psi$	Umbral cone half-angle

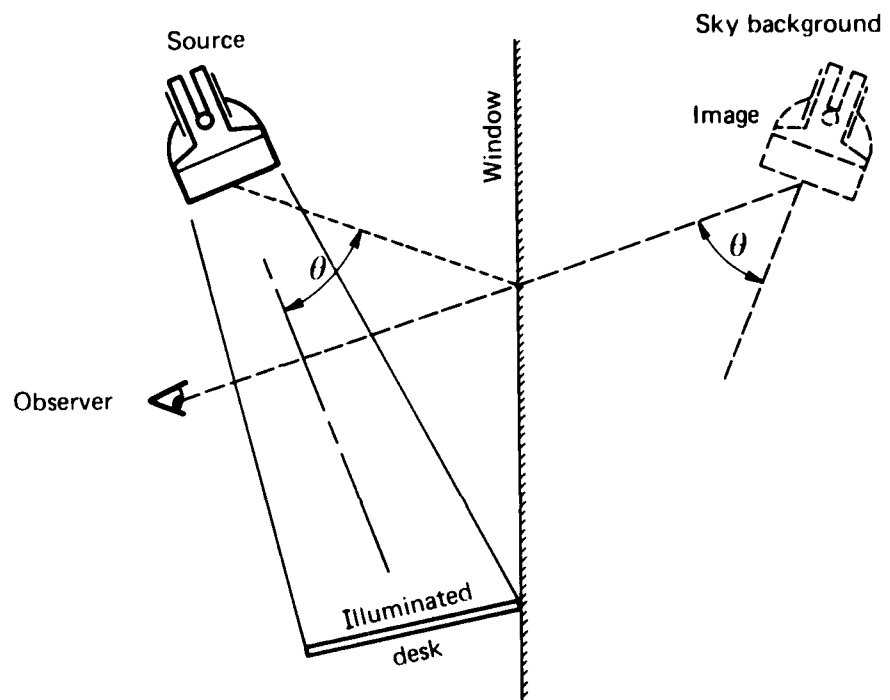


FIG. 1 UNWANTED IMAGE OF LIGHT SOURCE IN WINDOW

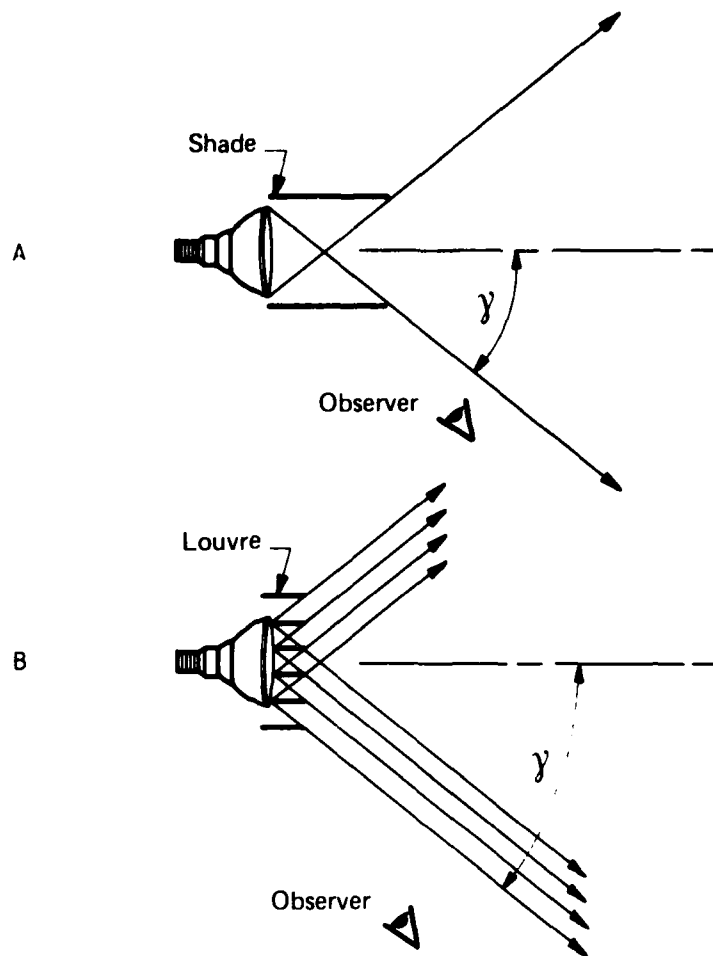


FIG. 2 EMITTING FACE OF LAMP NOT VISIBLE TO OBSERVER SHOWN BECAUSE OF ACTION OF CYLINDRICAL SHADE IN A, OR LOUVRE IN B, IN LIMITING DIRECT RAYS TO WITHIN A CONE OF SEMI-ANGLE  $\gamma$  ABOUT THE LAMP AXIS

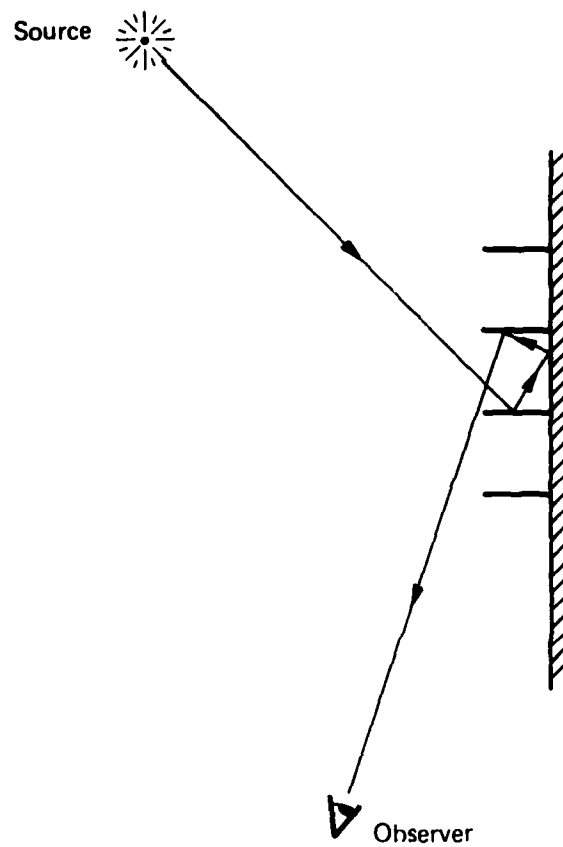


FIG. 3 THE EFFECT OF A LIGHT TRAP IN REDUCING REFLECTED LIGHT

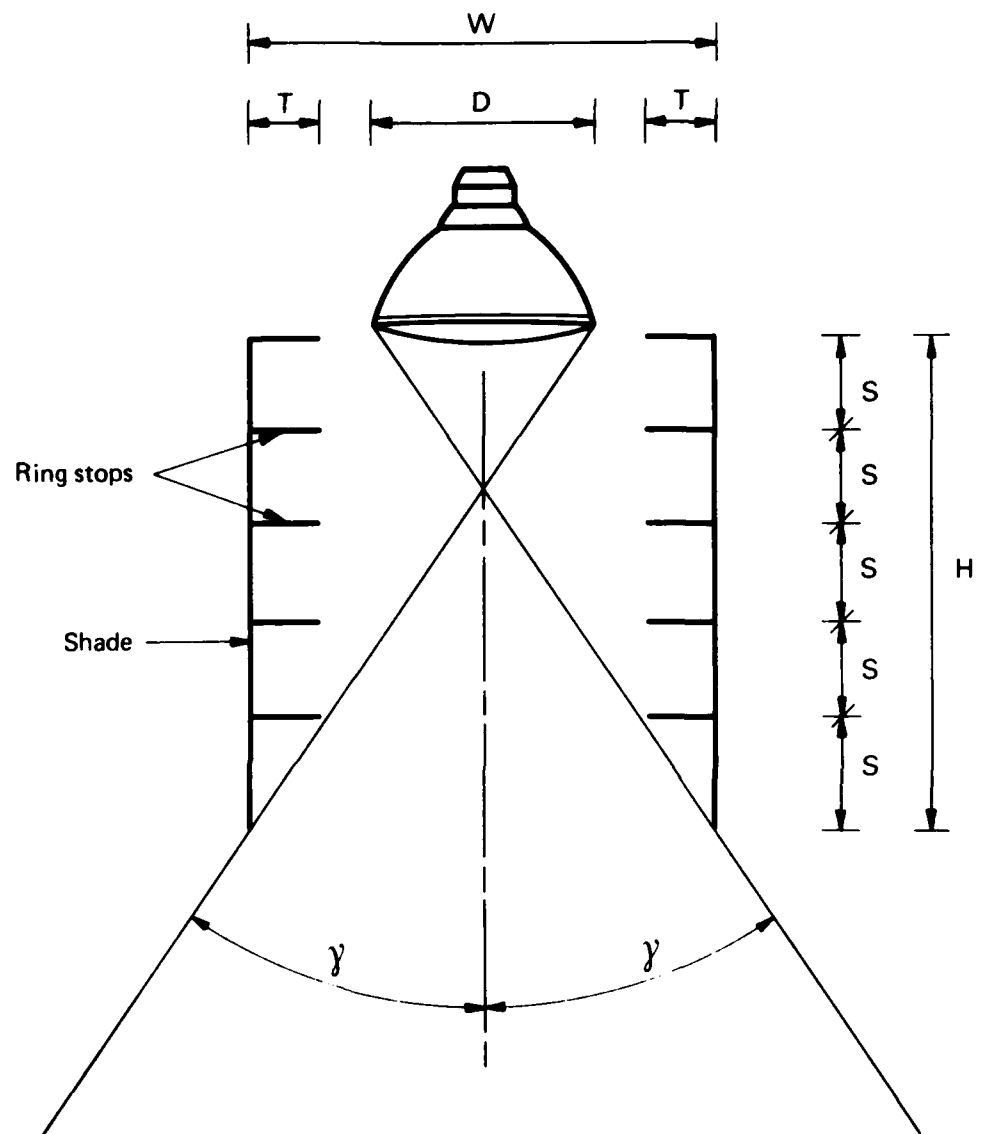


FIG. 4 GEOMETRY OF A SPOTLAMP BAFFLE (5 RINGS SHOWN)

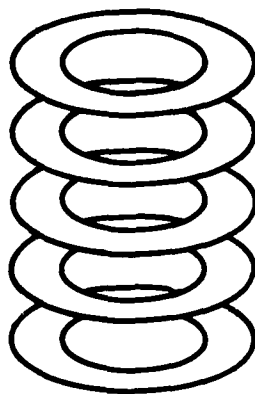


FIG. 5 PERSPECTIVE OF RINGS WITHOUT OUTER CASING

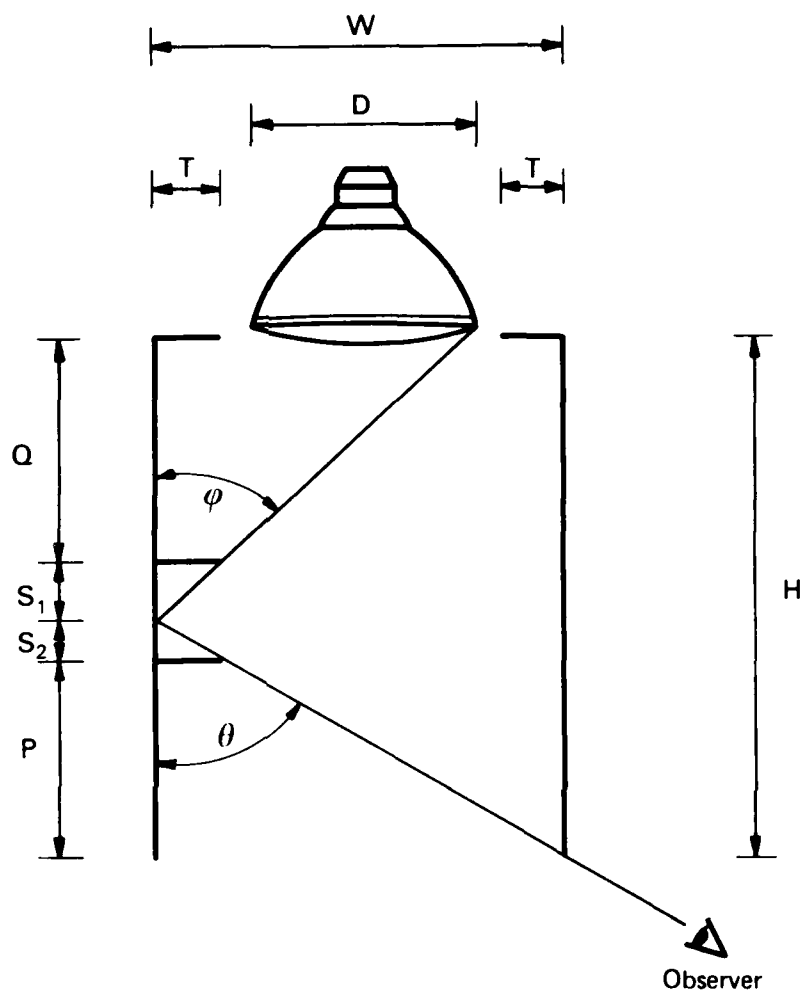


FIG. 6 GEOMETRY OF SPOTLAMP BAFFLE FOR CALCULATING SPACING BETWEEN STOPS



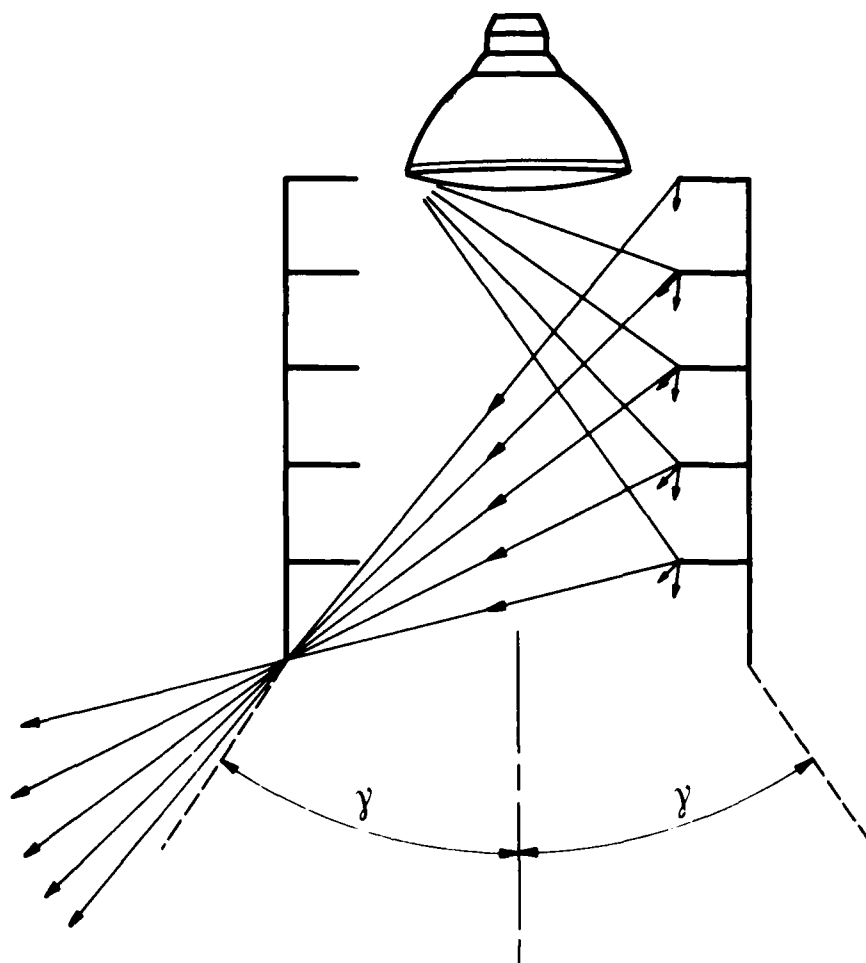


FIG. 7 REFLECTIONS FROM EDGES OF RING STOPS CAN ENABLE RAYS TO EXCEED CUT-OFF ANGLE,  $\gamma$

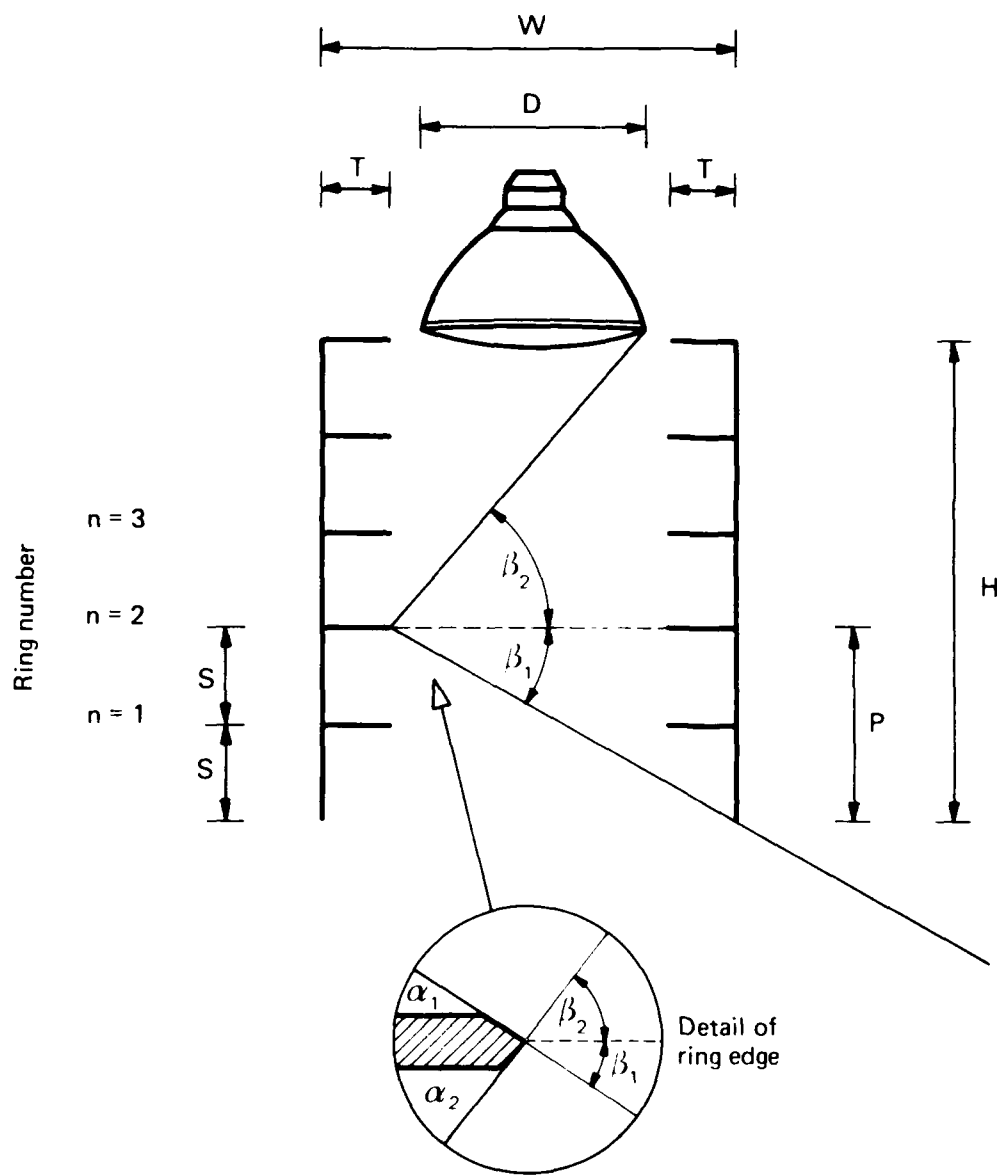


FIG. 8 ANGLES FOR SHARP EDGES

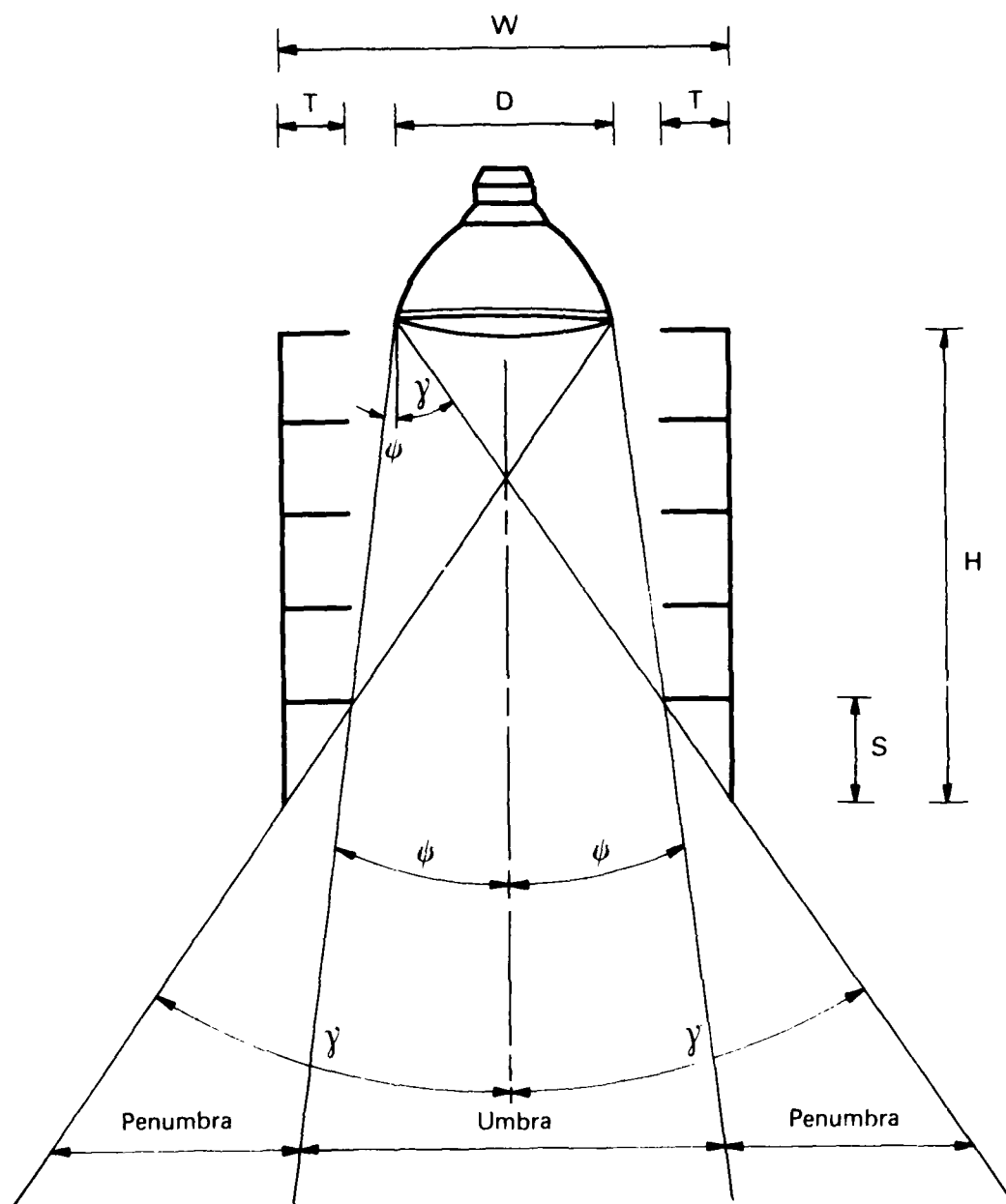


FIG. 9 UMBRA AND PENUMBRA REGIONS

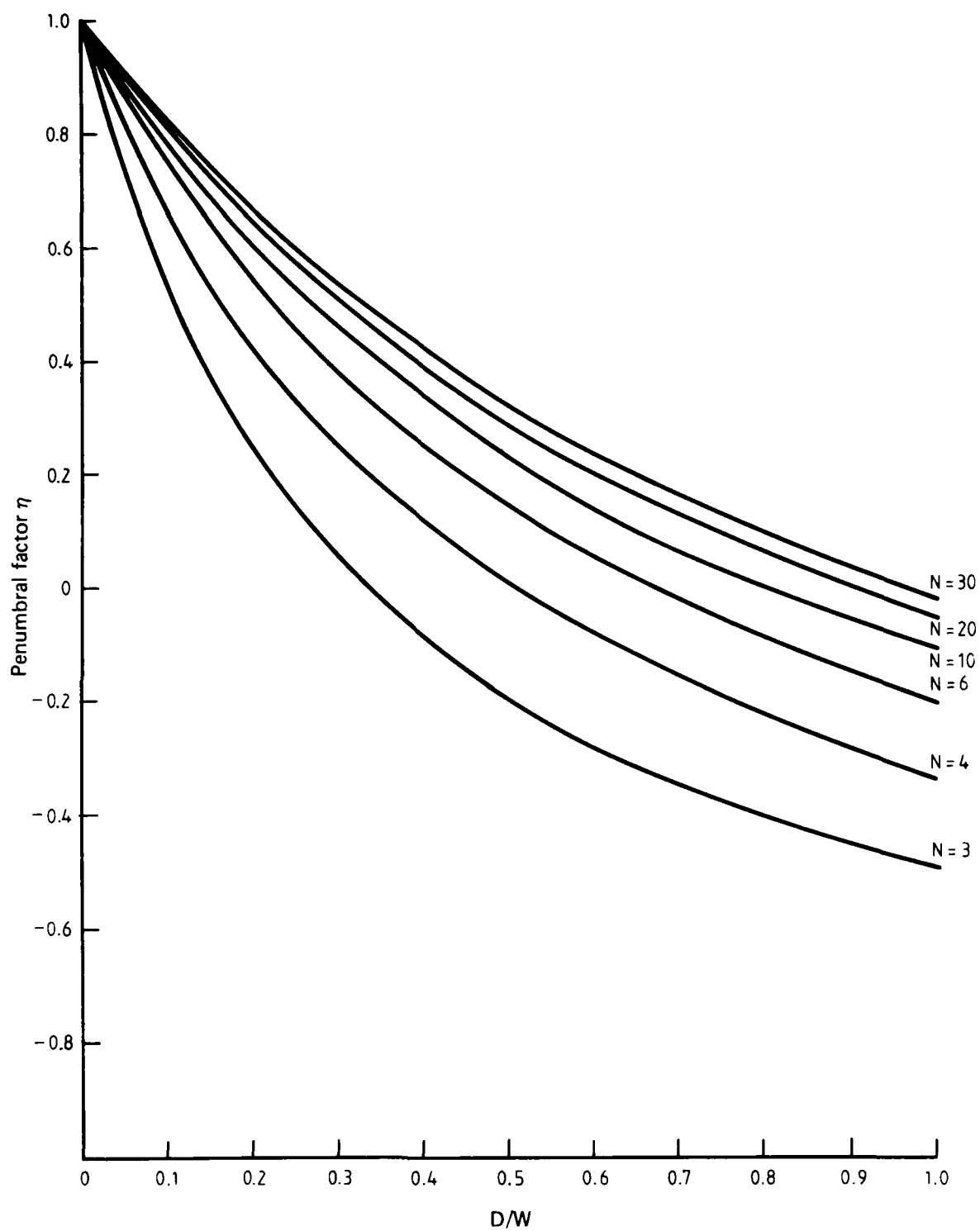


FIG. 10 THE PENUMBRAL FACTOR AS A FUNCTION OF  $N$  AND  $D/W$

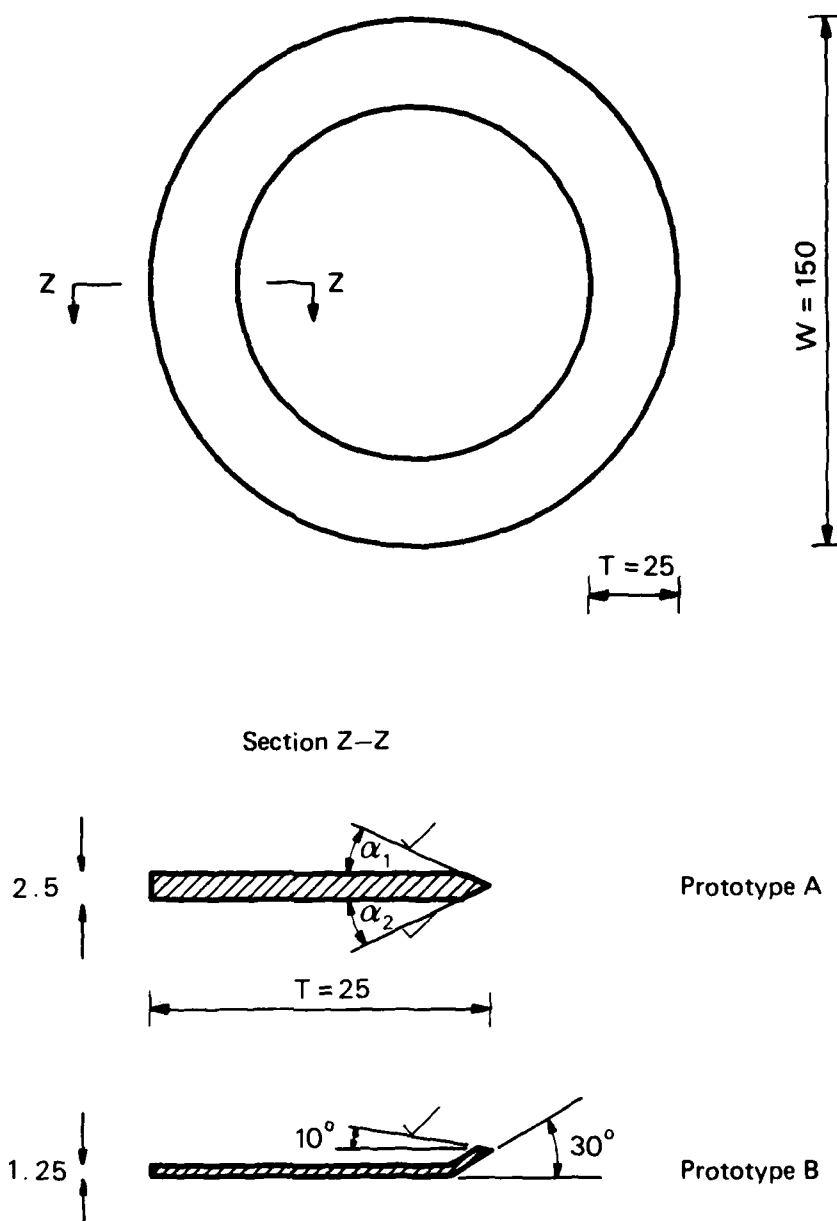


FIG. 11 RING SECTIONS OF ARL PROTOTYPE BAFFLES

✓ Denotes machined surfaces

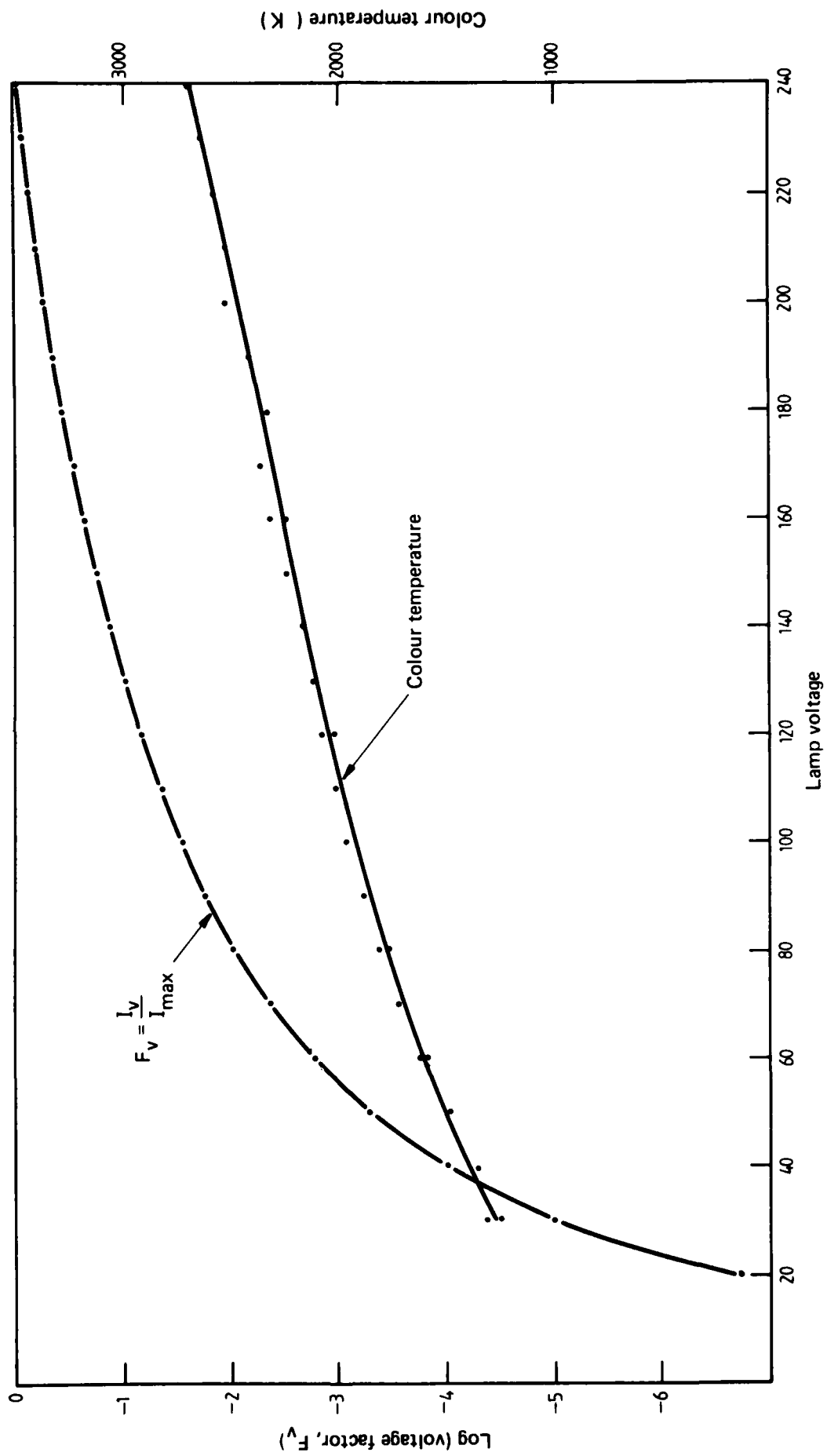


FIG 12 VOLTAGE EFFECT ON PAR 38 LAMP

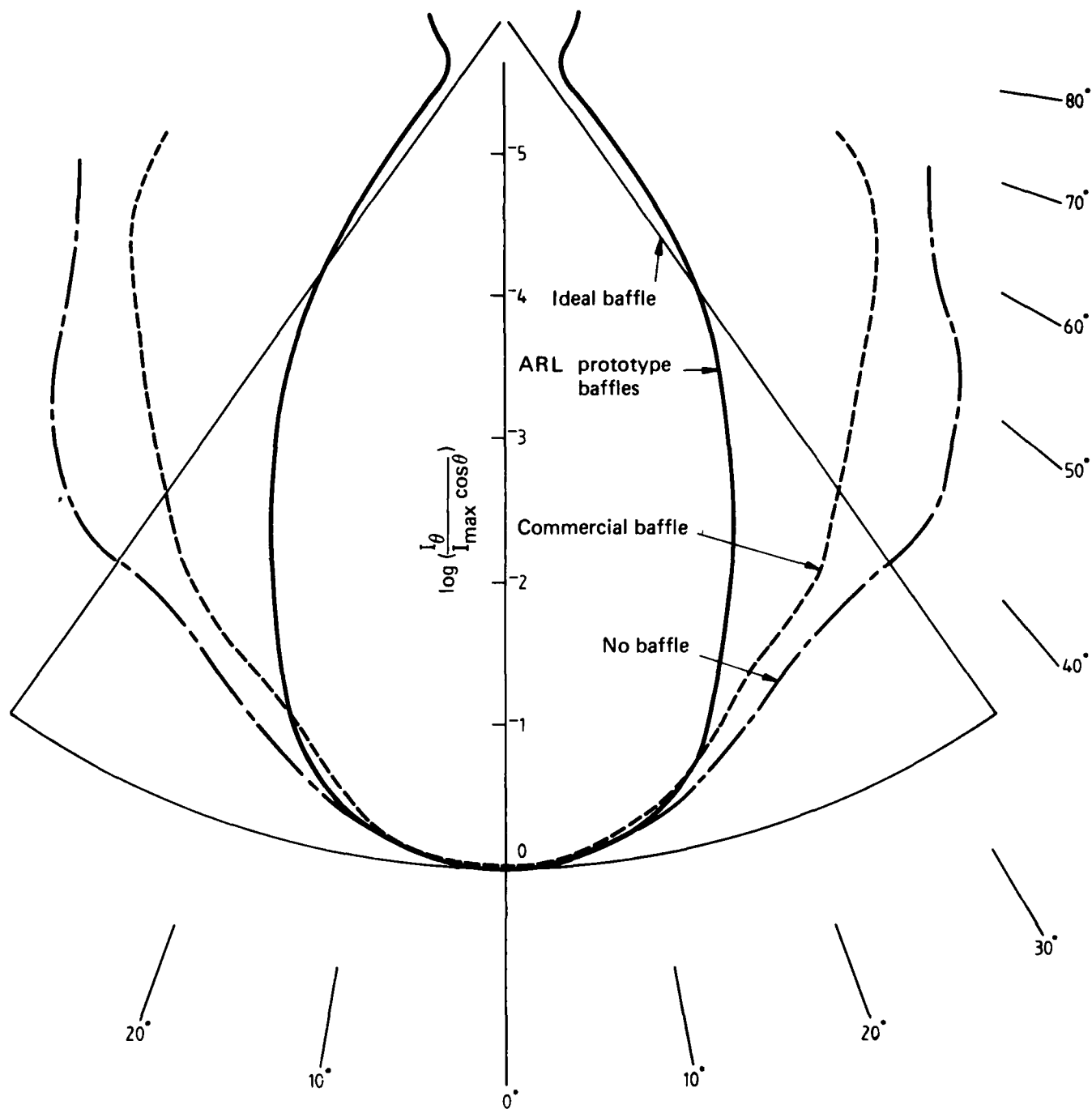


FIG. 13 SHADING EFFECT OF VARIOUS BAFFLES: POLAR PLOT OF ANGLE FACTOR

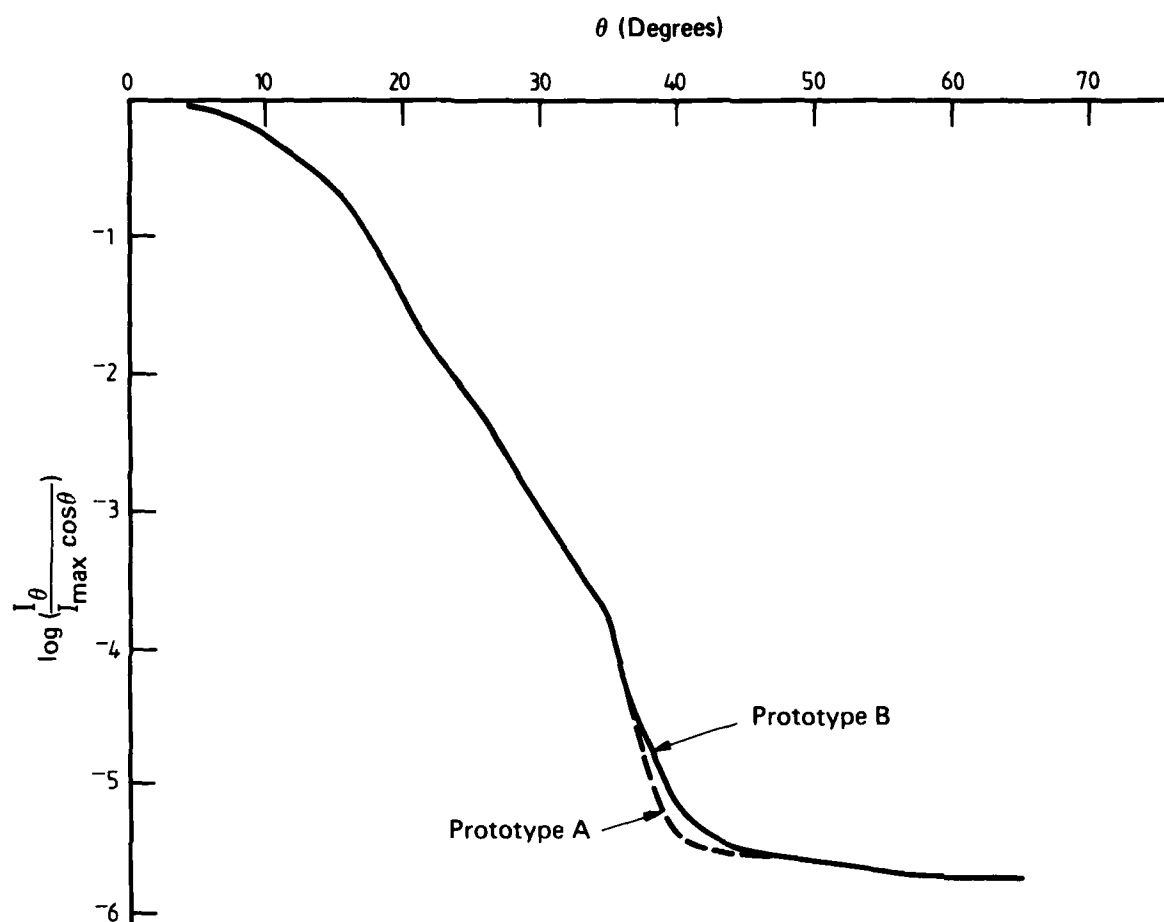


FIG. 14 PERFORMANCE DIFFERENCE BETWEEN PROTOTYPE BAFFLES:  
RECTANGULAR PLOT OF ANGLE FACTOR



## APPENDIX A

### Geometry of the Spotlight Baffle

The spotlight baffle is a cylinder of length  $H$  and width  $W$  with internal flat ring stops of uniform width  $T$  as shown in Figures 4 and 5. The diameter of the light-emitting face of the lamp is  $D$ . The clear aperture of the baffle is given by  $(W - 2T)$  which generally will be different from  $D$ .

#### 1. Cut-off Angle

Figure 4 shows the direct ray paths at the maximum angle at which any part of the emitting face of the lamp can be seen, i.e. the cut-off angle,  $\gamma$ . This is determined geometrically by a line joining one extreme edge of the light source to a point on the lower inside edge of the baffle on the opposite side. It is clear that this angle is given by

$$\tan \gamma = \left( \frac{D + W}{2H} \right). \quad (A1)$$

#### 2. Spacing

To determine the maximum axial spacing,  $S$ , between adjacent stops or fins of the light trap, consider the geometry shown in Figure 6.

Imagine a cylindrical shade initially with no ring stops. Then to any given point on the inside surface of the cylinder, a ray is drawn from that point on the lamp face which maximises the incident angle  $\phi$ . A second line (to represent a ray diffusely reflected at a maximum value of the angle  $\theta$  to an observer) is drawn just clear of the lower edge of the shade as shown. Opaque stops of dimension  $T$  are then located so as to touch those lines. This will ensure that the region dimensioned  $S_1$  cannot be illuminated directly by the source, and the region dimensioned  $S_2$  is always obscured from the observer's view.

From consideration of similar triangles containing the angle  $\phi$ ,

$$\frac{S_1}{S_1 + Q} = \frac{T}{W/2 + D/2},$$

and therefore

$$S_1 = \frac{2TQ}{W + D - 2T}. \quad (A2)$$

From similar triangles containing the angle  $\theta$ ,

$$\frac{S_2}{S_2 + P} = \frac{T}{W},$$

and because

$$S_2 + P = H - Q - S_1,$$

it follows that

$$S_2 = \frac{T}{W}(H - Q - S_1). \quad (A3)$$

The maximum spacing between stops which can still prevent observation via a single diffuse reflection is therefore  $S_1$  plus  $S_2$ . Using (A2) and (A3) this spacing,  $S_{\max}$ , is

$$S_{\max} = \frac{2TQ}{W + D - 2T} + \frac{T}{W} \left( H - Q - \frac{2TQ}{W + D - 2T} \right)$$

which reduces to

$$S_{\max} = \frac{TH}{W} + \frac{TQ}{W} \frac{(W - D)}{(W + D - 2T)} \quad (\text{A4})$$

As the parameter  $Q$  varies through a series of values from zero for the uppermost ring stop to  $(H - S_1)$  for the ring stop farthest from the lamp, the above formula indicates that  $S_{\max}$  varies through a corresponding series of values from

$$\left( \frac{TH}{W} \right) \text{ to } \left( \frac{2TH}{W + D} \right).$$

A constant spacing between ring stops may be desirable for ease of manufacture and the spacing therefore should not exceed the smaller of these, viz.:

$$S = \frac{TH}{W} \quad (\text{A5})$$

The number of ring stops is one fewer than the number of spacings,  $N$ , which is determined by the baffle length,  $H$ , divided by the spacing between adjacent ring stops, and rounding up if necessary. Therefore if  $S$  is determined by equation (A5),

$$\frac{W}{T} + 1 > N \geq \frac{W}{T} \quad (\text{A6})$$

When  $W/T$  is selected to be an integer,

$$N = \frac{W}{T} \quad (\text{A7})$$

Should the constant spacing be used, the ring stop farthest from the lamp will be closer to the shade rim than necessary. The cut-off angle will then be determined by the location of the inner edge of that ring stop. The value for the cut-off angle would then be

$$\gamma = \arctan \frac{(W + D - 2T)}{2(H - S)} \quad (\text{A8})$$

which would be only a little smaller than the value given in (A1) above.

### 3. Angles for Sharp Edges

The angles  $\beta_1$  and  $\beta_2$  are defined in Figure 8 and can be determined geometrically as follows:

$$\tan \beta_1 = \frac{P}{W - T}$$

and

$$\tan \beta_2 = \frac{2(H - P)}{W + D - 2T}$$

Because  $P = nS$  where  $n$  is the ring number from the outer end ( $n = 1$  to  $(N - 1)$ ) as shown in Figure 8, and using  $S$  from Equation (A5), the first of these becomes

$$\tan \beta_1 = \left( \frac{n}{W - T} \right) \left( \frac{TH}{W} \right).$$

Using Equation (A7), this reduces to

$$\tan \beta_1 = \frac{n}{N} \left( \frac{H}{W - T} \right) \quad (\text{A9})$$

and similarly

$$\tan \beta_2 = \left(1 - \frac{n}{N}\right) \left(\frac{2H}{W + D - 2T}\right). \quad (\text{A10})$$

#### 4. Penumbra Region

The umbral region is formed by a cone defined to include the circular periphery of the lamp's emitting face and the circular inner edge of the ring stop farthest from the lamp. As seen in Figure 9, the umbral cone has a half-angle,  $\psi$ , which is determined by

$$\tan \psi = \frac{(W/2 - D/2 - T)}{(H - S)}. \quad (\text{A11})$$

The Penumbra Factor,  $\eta$ , defined as

$$\eta = \frac{\tan \psi}{\tan \gamma},$$

can be expanded using equations (A8) and (A11) to

$$\eta = \left(\frac{W - D - 2T}{W + D - 2T}\right).$$

Using (A7) in order to express  $T$  in terms of the number of spacings,  $N$ , it follows that

$$\eta = \left(\frac{W - D - 2W/N}{W + D - 2W/N}\right)$$

which reduces to

$$\eta = \frac{1 - D/W - 2/N}{1 + D/W - 2/N}. \quad (\text{A12})$$

This relationship is shown graphically in Figure 10.

## APPENDIX B

### Spotlamp Data

Trade name:	Philips Cool-spot 'Attralux' PAR 38
Description:	220-240 V, 150 W incandescent pressed-glass lamp with spherical-paraboloidal dichroic reflector
	Overall diameter 121 mm
	Overall length 133 mm
	Edison screw 27 mm cap
Total luminous output at rated voltage:	1600 to 1700 lumen
Intensity at rated voltage:	7000 cd on axis 5000 cd at 5° off axis 3500 cd at 8° off axis 3000 cd at 10° off axis 2000 cd at 15° off axis
Illuminance on axis at rated voltage:	2800 lux at 1.5 m 1120 lux at 2.5 m 570 lux at 3.5 m
Maximum luminance of emitting surface at rated voltage:	$6.2 \times 10^5 \text{ cd m}^{-2}$

## **APPENDIX C**

**Photographs of Lamp, Shades and Rings**

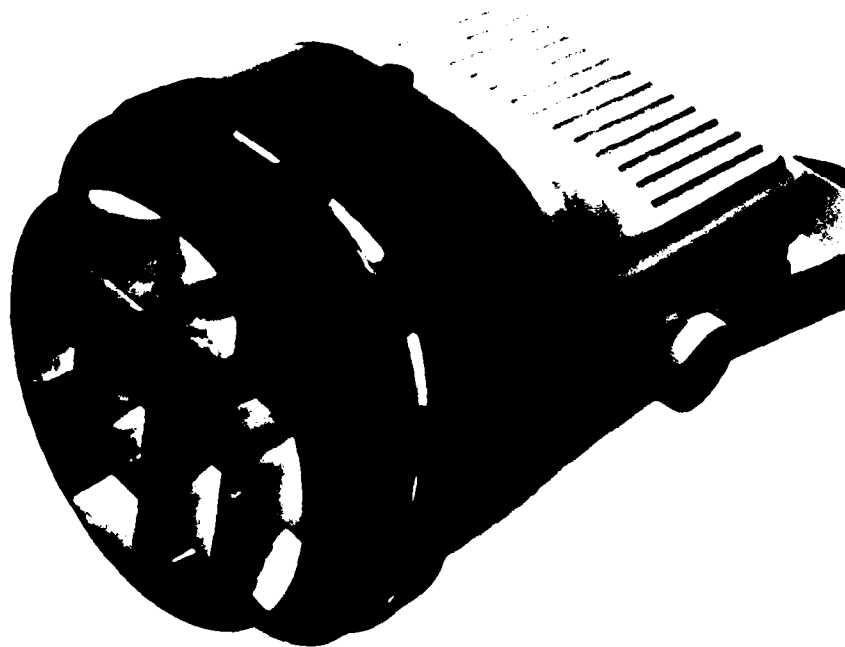


FIG. C1 LAMP HOUSING WITH COMMERCIAL GRID TYPE LOUVRE SHADE

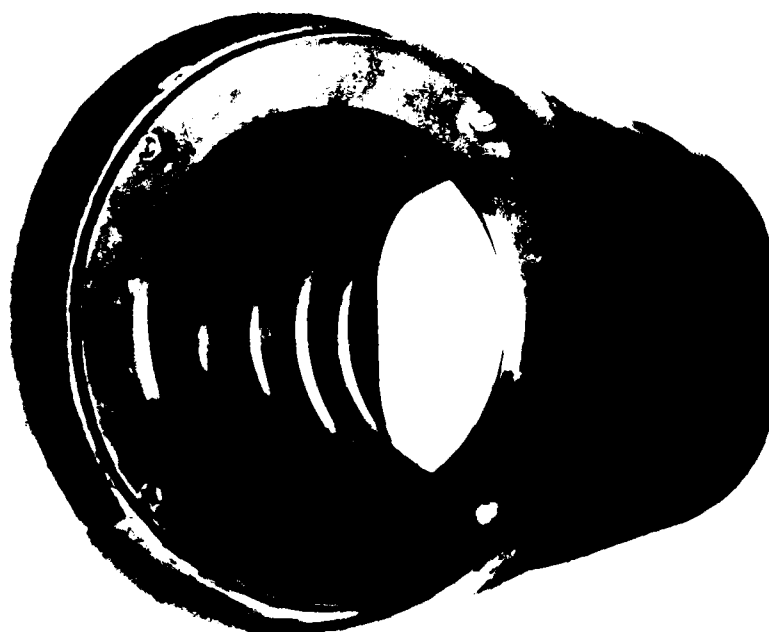


FIG. C2 ARL BAFFLE (PROTOTYPE A)

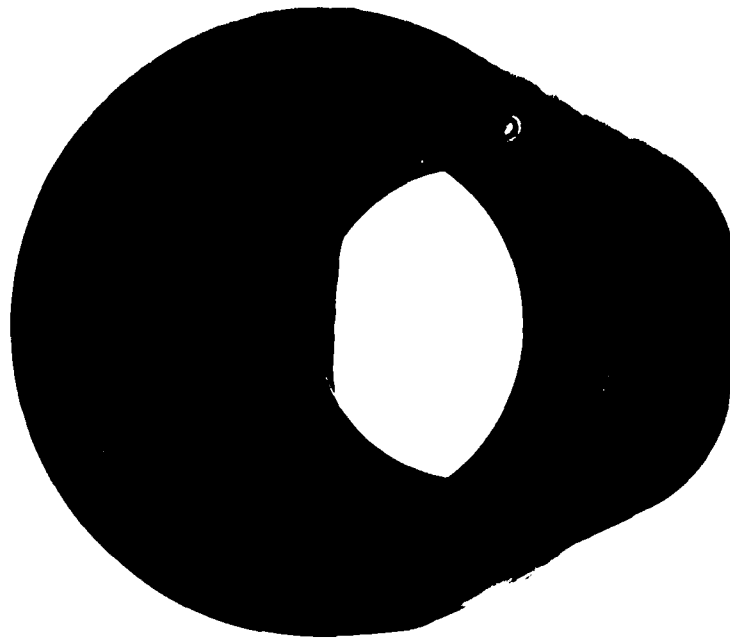


FIG. C3 ARL BAFFLE (PROTOTYPE B)



FIG. C4 SAMPLE RING SECTION (PROTOTYPE A)



FIG. C5 SAMPLE RING SECTION (PROTOTYPE B)



## DISTRIBUTION

Copy No.

### AUSTRALIA

#### Department of Defence

##### Central Office

Chief Defence Scientist	1
Deputy Chief Defence Scientist	2
Superintendent, Science and Technology Programs	3
Australian Defence Scientific and Technical Representative (UK)	—
Counsellor, Defence Science (USA)	—
Joint Intelligence Organisation	4
Defence Library	5
Document Exchange Centre, DISB	6-22
DGAD (NCO)	23

##### Aeronautical Research Laboratories

Chief Superintendent	24
Library	25
Superintendent—Systems Division	26
Divisional File—Systems	27
Cybernetics Group File	28
Authors: K. W. Anderson	29
B. A. J. Clark	30

##### Materials Research Laboratories

Library	31
Optics Group	32

##### Defence Research Centre, Salisbury

Library	33
---------	----

##### Central Studies Establishment

Information Centre	34
--------------------	----

##### RAN Research Laboratory

Library	35
---------	----

##### Defence Regional Office

Library	36
---------	----

##### Navy Office

Naval Scientific Adviser	37
Director, Naval Ship Design	38
Director, Naval Aviation Policy	39
OC, HMAS <i>Albatross</i>	40-42
OC, HMAS <i>Melbourne</i>	43

##### Army Office

Army Scientific Adviser	44
Royal Military College, Library	45
US Army Standardisation Group	46

<b>Air Force Office</b>	
Aircraft Research and Development Unit, Scientific Flight Group	47
Air Force Scientific Adviser	48
Technical Division Library	49
DGAIRENG	50
HQ Operational Command	51
Director General Operational Requirements—AF	52
<b>Department of Industry and Commerce</b>	
Government Aircraft Factories:	
Manager	53
Library	54
<b>Department of Science and Technology</b>	
Bureau of Meteorology, Publications Officer	55
<b>Department of Transport</b>	
Secretary	56
Library	57
Planning, Research and Development Branch	58
<b>Statutory, State Authorities</b>	
CSIRO, Mechanical Engineering Division, Chief	59
CSIRO, National Measurement Laboratory, Chief	60
SEC of Victoria, Herman Research Laboratory, Librarian	61
SEC of Queensland, Library	62
<b>Universities and Colleges</b>	
Adelaide Barr Smith Library	63
Flinders Library	64
James Cook Library	65
La Trobe Library	66
Melbourne Engineering Library	67
Optometry Library	68
Monash Library	69
Newcastle Library	70
New England Library	71
Sydney Engineering Library	72
New South Wales Library	73
Queensland Library	74
Tasmania Engineering Library	75
Western Australia Library	76
RMIT Library	77
<b>CANADA</b>	
CAARC Coordinator, Human Engineering	78
International Civil Aviation Organization, Library	79
Defence and Civil Institute of Environmental Medicine, Head, Behavioural Sciences Division	80
<b>FRANCE</b>	
AGARD, Library	81
<b>INDIA</b>	
CAARC Coordinator, Human Engineering	82
Civil Aviation Department, Director	83
National Aeronautical Laboratory, Director	84
<b>JAPAN</b>	
National Aerospace Laboratory, Library	85

<b>NETHERLANDS</b>	
Central Org. for Applied Science Research TNO, Library	86
National Aerospace Laboratory (NLR), Library	87
<b>NEW ZEALAND</b>	
Defence Scientific Establishment, Librarian	88
Transport Ministry, Civil Aviation Division, Library	89
OC DEMU	90
CAARC Coordinator, Human Engineering	91
<b>SWEDEN</b>	
Aeronautical Research Institute	92
<b>UNITED KINGDOM</b>	
CAARC, Secretary	93
Royal Aircraft Establishment:	
Farnborough, Library	94
Bedford, Library	95
National Physical Laboratories, Library	96
British Library, Science Reference Library	97
CAARC Coordinator, Human Engineering	98
Science Museum Library	99
Imperial College, The Head	100
<b>UNITED STATES OF AMERICA</b>	
NASA Scientific and Technical Information Facility	101
American Institute of Aeronautics and Astronautics	102
Spares	103-132

